J Mol Model (2012) 18:3507–3522
DOI 10.1007/s00894-011-1348-1

ORIGINAL PAPER

Ab initio and density functional theoretical design and screening of model crown ether based ligand (host) for extraction of lithium metal ion (guest): effect of donor and electronic induction

Anil Boda · Sk. Musharaf Ali · Hanmanth Rao · Sandip K. Ghosh

Received: 27 September 2011 / Accepted: 22 December 2011 / Published online: 10 February 2012

Abstract The structures, energetic and thermodynamic parameters of model crown ethers with different donor, cavity and electron donating/ withdrawing functional group have been determined with *ab initio* MP2 and density functional theory in gas and solvent phase. The calculated values of binding energy/ enthalpy for lithium ion complexation are marginally higher for hard donor based aza and oxa crown compared to soft donor based thia and phospha crown. The calculated values of binding enthalpy for lithium metal ion with 12C4 at MP2 level of theory is in good agreement with the available experimental result. The binding energy is altered due to the inductive effect imparted by the electron donating/ withdrawing group in crown ether, which is well correlated with the values of electron transfer. The role of entropy for extraction of hydrated lithium metal ion by different donor and functional group based ligand has been demonstrated. The HOMO-LUMO gap is decreased and dipole moment of the ligand is increased from gas phase to organic phase because of the dielectric constant of the solvent. The gas phase binding energy is reduced in solvent phase as the solvent molecules weaken the metal-ligand binding. The theoretical values of extraction energy for LiCl salt from aqueous solution in different organic solvent is validated by the experimental trend. The study presented here should contribute to the design of model host ligand and screening of solvent for metal ion recognition and thus can contribute in planning the experiments.

Keywords *Ab initio* · Crown ether · Design and screening of ligand · DFT · Molecular modeling · Solvent extraction

Introduction

Naturally occurring lithium isotope consists of two stable isotopes, ^{6}Li & ^{7}Li, and each isotope plays an important role in nuclear science and industry[1, 2]. ^{7}Li can be used as a coolant in nuclear fission reactors [3]. Also, isotopically pure ^{7}LiOH is used to adjust the pH of the primary coolant of a pressurized water reactor [4]. Li^{+} is used in the medical field as a therapeutic agent for the treatment of manic depression [5, 6]. In the future, lithium compounds rich in ^{6}Li will be required for the tritium breeder blanket in deuterium-tritium fusion power reactors [7]. These are just a few of the many applications and potential areas where the use of Li metal ion/ isotopes is of crucial importance. Therefore, their physical separation, or at least detection, is an important endeavor. Various methods for lithium isotope separation have been developed, and their application to large-scale enriched lithium isotope production has been assessed. Any chemical exchange process with a separation factor (α) >1.04 will be of practical interest. In that context, special attention has been paid to the use of crown ether,

Electronic supplementary material The online version of this article (doi:10.1007/s00894-011-1348-1) contains supplementary material, which is available to authorized users.

A. Boda · S. M. Ali (✉) · H. Rao
Chemical Engineering Division, Bhabha Atomic Research Centre, Mumbai 400 085, India
e-mail: musharaf@barc.gov.in

S. K. Ghosh
Chemical Engineering Group, Bhabha Atomic Research Centre, Mumbai 400 085, India

which are recently been used as a promising separating agent from a mixture of different isotopes having very small difference in size [8, 9]. So it will be worthwhile to explore the underlying mechanism of complexation of lithium metal ion with crown ligand of different donor, cavity and electron withdrawing and electron donating functional group in gas as well as in the organic solvent phase.

Macrocyclic crown ethers [10], due to its selective binding affinity acts as a host for various neutral or charged solutes especially the metal ions as guest within its nano cavity. This highly specific host-guest chemistry has been exploited in the ligand design for various applications: such as metal ion separation from nuclear and chemical waste [11, 12], isotope separation [13], ion recognition [14], phase transfer catalyst [15], molecular electronic switch [16]. The interaction of host crown ether moiety with guest molecules arises due to the interaction of charge (metal ion) and dipole (arises from the donor atom in crown ether). This host-guest interaction can be tuned for a specific guest metal ion by altering the orientation of the donor atom, cavity size, type of donor atom (soft or hard) and substitution of electron withdrawing or electron donating group. Another crucial factor is the solvent which plays a decisive role in changing the host-guest interaction and hence control the selectivity and transport of the guest metal ions. Once a ligand is designed based on the host-guest interaction, its use is to be tested in the practical application such as separation of metal ion from aqueous solution to an immiscible desired solvent phase. Hence, aqueous solubility and partition coefficients of the designed ligand in bi-phasic water-organic system are also very crucial from practical application point of view.

Extensive study on metal ion crown ether system has been reported at various level of electronic structure theory [17–44]. Recently, studies have been performed on the effect of cavity size, microsolvation and substitution on the metal ion-crown ether interaction for metal ion selectivity [45, 46]. Donor atom of the host ligand also plays a very decisive role on the interaction and hence in the selectivity and transport of the metal ion. The effect of donor atom on the metal ion-crown ether system has been started recently. In that context, DFT study was carried out to explain the selectivity of Aza-12C4 for Li, Na and K using DZVP basis set [47]. The stable structures of Aza-12C4 and its complexes with Li and Na in solvent has been reported at B3LYP/6-31 G**//RHF/6-31-G* level of theory [48]. The binding selectivity of Li^+, Na^+ and Be^{2+} with 12C4 crown ether with N, P and S as donor atom has been studied at B3LYP/6-31+G** level of theory [49, 50].

The reported studies on donor atom were mainly concentrated to DFT level of theory with low basis set and 12 member crown ring only. The objectives of the present work are manifold, namely: (i) effect of type (soft/hard) of donor atom on the ligand structure and ligand–metal ion interaction (ii) to extend the donor atom effect on large cavity based crown ether such as 15 and 18 member crown rings (number of donor atom decides the cavity size) (iii) effect of electron donating and electron withdrawing functional group on the structure and interaction (iv) solvent effect on the structure and interaction of crown ether ligand with metal ion (v) solubility of the crown ethers in water and finally the partition coefficients of the designed crown ether in different water-organic biphasic system. This is a modest attempt to present a workable scheme for the design and screening of ligand-solvent system for Li metal ion extraction from aqueous solution purely on computational means.

Details of the computational methodologies are provided in Sect. II. The results are then discussed in Sect. III and finally conclusion is drawn in Sect. IV.

Computational experiment

It is well known that Hartree-Fock (HF) does not consider the electronic correlation in the calculation. Density functional theory (DFT) though it considers the correlation it uses the fitted functional in the calculation, whereas Moller-Plesset second order perturbation (MP2) [51] level of theory considers the electronic correlation in the calculation. Hence, all the calculations have been performed at the MP2 level of theory using all electrons 6-311+G (d, p) basis set. The calculations have been carried out using frozen core approximation to speed up the calculation in view of the floppy nature of the crown ethers system. The calculated values of binding enthalpy for lithium metal ion with 12C4 at MP2 level of theory (-84.76 kcal mol^{-1}) is in good agreement with the experimental [52] data (-90± 12 kcal mol^{-1}). To further test the predictability of the present methodology, we have optimized the structure of B12C4-LiCl complex. The calculated Li-O (2.043 Å) and Li-Cl (2.15 Å) distances are in good agreement with the crystallographic data (2.12 Å and 2.29 Å respectively) [53]. The optimized equilibrium structure has been obtained using initial guess structures obtained from our earlier study followed by full geometry optimizations based on Newton Rapson optimization scheme as implemented in GAMESS [54] suit of electronic structure calculation code.

The true stationary structures are assured for all the optimized equilibrium structures through Hessian calculations. Hessian calculations are also used for the estimation of thermodynamic parameters. MOLDEN graphics program was used for the visualization of various molecular geometries and associated structural parameters [55].

Macrocyclic crown ethers with narrow cavity are excellent host in trapping charged metal ions; hence the most

important property to be studied is the gas phase binding energy (BE). The B.E (ΔE) of the metal ion (M^+)-crown ether ligand (L) complexation reaction,

$$M^+ + L = M^+L, \quad (1)$$

is defined by the following general relation,

$$\Delta E = E_{M^+\text{-ether}} - (E_{M^+} + E_{ether}), \quad (2)$$

where, $E_{M^+\text{-ether}}$, E_{M^+} and E_{ether} refer to the energy of M^+-ether complex, M^+ ion and the free ether system respectively.

The thermal correction to the electronic energy (E_{el}), enthalpy (H) and free energy (G) of the optimized hydrated cluster has been performed to predict the thermodynamic parameters [56]. The thermal and zero point energy corrected binding energy is

$$\Delta U = U_{M^+\text{-ether}} - (U_{M^+} + U_{ether}), \quad (3)$$

where $U_{M^+\text{-ether}}$, U_{M^+} and U_{ether} represent the internal energy of the M^+-ether complex, M^+ ion and the free ether system respectively.

The binding enthalpy (ΔH) and binding free energy (ΔG) for the metal ion-crown ether complexation reaction in Eq. (1) are calculated using the following standard thermodynamic relation

$$\Delta H = \Delta U + \Delta nRT. \quad (4)$$

$$\Delta G = \Delta H - T\Delta S. \quad (5)$$

In order to explore the effect of hydrated metal ion which is a realistic picture from the experimental point of view we have also calculated the enthalpy and free energy of the following exchange reaction:

$$Li^+ - (H_2O)_n + L \rightarrow Li^+ - L + nH_2O (n = 1 - 6). \quad (6)$$

Most of the metal ion extraction takes place from the aqueous solution phase to the organic solvent phase. Hence, the consideration of solvent effect on the structure and complexation of the ligand moiety with metal ion is of utmost importance. The inclusion of the solvent in the QM calculation is thus indispensable. In order to study the solvent effect, the optimized geometry obtained from MP2 level of theory has been reoptimized using conductor like screening model (COSMO) at DFT [57] level of theory with generalized gradient approximated BP-86 using triple zeta valence plus polarization (TZVP) basis set as implemented in TURBOMOLE quantum chemistry package [58]. BP-86 functional is a combination of Becke B88 exchange functional [59] and Perdew P86 correlation functional [60] and was found to be successful in predicting molecular properties. The solubility and partition coefficients of the designed model ligand is calculated using statistical thermodynamics as incorporated in COSMOtherm molecular modeling software [61].

In quantum electronic structure calculation the solvent effect is incorporated through the most popular COSMO-RS real solvent model [62–65]. The basic idea behind this model is to divide the solute surface segment into a large number of discrete smaller surfaces. Each surface segment is characterized by its area a_i and the screening charge density (SCD, it is the screening of the solute's charge by virtual conductor, i.e., the surrounding environment along with the back polarization) is characterized by σ_i . When two such molecular surfaces come into contact they lead to some electrostatic interaction energy. These microscopic surface interaction energies can be used to predict the macroscopic thermodynamic properties using statistical thermodynamics. The probability distributions ($p^X(\sigma)$) of σ for any compound X_i is called σ profile and the corresponding chemical potential for a surface segment with SCD is called σ-potential and is given by:

$$\mu_S(\sigma) = -RT\ln\left[\int p_S(\sigma')\exp\{(\mu_S(\sigma') - a_{eff}e(\sigma,\sigma'))/RT\}d\sigma'\right] \quad (7)$$

The chemical potential of compound X_i in system S is given by:

$$\mu_S^{Xi} = \mu_{C,S}^{Xi} + \int p^{Xi}(\sigma')\mu_S(\sigma')d\sigma \quad (8)$$

Here $\mu_{C,S}^{Xi}$ is a combinatorial contribution to the chemical potential. The chemical potential μ_S^{Xi} is used for the evaluation of the activity coefficients of the solute in the solvent or solvent mixture by the expression as: [66]

$$\gamma_S^X = \exp\{-(\mu_S^X - \mu_X^X)/K_BT\}. \quad (9)$$

The solubility, S_S^X of a solute (X) in a solvent (S) then can be calculated using the following expression: [67]

$$S_S^X = \exp\{-[\mu*_S^X - \mu*_X^X + RT\ln v_S]/RT\}, \quad (10)$$

where, $\mu*_S^X = \mu_S^X - RT\ln x_S^X$. Here, x_S^X is the molar concentration of compound X in solvent S and v_S is the molar volume of the solvent.

Similarly the partition coefficients of a solute j between two solvent (aqueous, w and organic, o) can be written as

$$\log K_j(o,w) = \log\{\exp[(\mu_j^w - \mu_j^o)/RT] * V_w/V_o\} \quad (11)$$

where V_w/V_o is volume quotient and can be evaluated either from experiment or COSMO-RS prediction [68].

The solvent extraction reaction for LiCl salt from aqueous to organic phase was modeled using the following reaction:

$$Li^{+}(aq) + Cl^{-}(aq) + L(org) \rightarrow L - LiCl(org), \quad (12)$$

to calculate the extraction energy as follows:

$$E_{ex} = E_{L-LiCl(org)} - \left(E_{L(org)} + E_{Li^{+}(aq)} + E_{Cl^{-}(aq)}\right). \quad (13)$$

Quantum electronic structure calculation has an extraordinary potential for calculating global and local indices that describe the inherent reactivity of chemical species quantitatively and is thus very useful to describe the host (crown ether) guest (metal ion) type interaction. Chemical systems are generally characterized by its electronic chemical potential, μ and absolute hardness, η and are defined as [69]:

$$-\mu = (I + A)/2 = \chi \quad \eta = (I - A)/2, \quad (14)$$

where I is the ionization potential and A is the electron affinity. Here, χ is called the absolute electronegativity. According to Koopmans' theorem [57], I and A can be obtained as

$$I = -E_{HOMO} \qquad A = -E_{LUMO} \quad (15)$$

If donor acceptor system is brought together, electrons will flow from that of lower χ to that of higher χ, until the chemical potentials become equal. The amount of charge transfer, ΔN can be calculated by applying the following formula [70]

$$\Delta N = (\chi_M - \chi_L)/\{2(\eta_M + \eta_L)\}. \quad (16)$$

Here, M stands for metal ion, which acts as Lewis acid, i.e., acceptor and L stands for ligand, i.e., crown ether, which acts as Lewis base, i.e., donor.

A higher value of E_{HOMO} indicates a tendency of the molecule to donate electrons to appropriate acceptor molecule of low empty molecular orbital energy. On the other hand, the energy of the lowest unoccupied molecular orbital indicates the ability of the molecule to accept electrons. Larger values of the energy difference, $\Delta E = E_{LUMO} - E_{HOMO}$, provide low reactivity to a chemical species and hence more stable and lower values of the energy difference indicates higher reactivity means less stable.

In order to test the validity of the theoretical scheme, solvent extraction experiment was also carried out. B12C4 (Aldrich make) was used as the extracting ligand for the solvent extraction experiment. Lithium chloride (SD fine chemical, India) was used to prepare the feed lithium salt solution with distilled water. Nitrobenzene, chloroform and CCl_4 were used as the organic solvent. Centrifuge machine was used for distinct phase separation of the solvent. Atomic absorption spectrophotometer (GBC make model Avanta), has been used for the concentration measurement. First the crown ether was washed with distilled water to remove any impurities from the crown ether. During the experiment, equal volume of the aqueous solution of the LiCl salt (2 M) is mixed with crown ether solution (0.186 M). The mixture was stirred for 30 minutes and depleted aqueous solution was separated from the crown ether using a separating funnel after phase separation using centrifuge. The metal ion trapped in crown ether is stripped by washing with water for several times. The enriched aqueous solution was concentrated. Both the enriched and depleted aqueous solution was analyzed by AAS to determine the concentration of the metal ion in the solution and hence to arrive at the value of distribution coefficient.

Results and discussion

The optimized structures of crown ethers and lithium ion-crown complexes, various structural and energy parameters, molecular descriptors and thermodynamic parameters with different ring size, donor atoms and functional group are presented here. The representative metal ion considered here for calculation is lithium due to its utmost significance in the field of nuclear science and technology. It is known that crown ethers have many conformers due to flexible single bond and orientation of donor atom. We will not dwell here for the generation of crown ethers conformers. Instead, we have taken the initial input coordinates of most stable 12C4, 15C5 and 18C6 from our earlier study [45, 46]. We believe that global minimum geometry will be close to this structure as the predicted structures reproduce the experimental data quite well. Details on the predicted structures and calculated results are provided in the following sections.

Geometrical parameters

Free crown ethers

The structure and subsequently the binding energy of metal-ligand system can be altered by varying the type and nature (soft or hard donating ability) of the donor atom. The optimized geometries of free crown ether with different donor atom at MP2 level of theory are displayed in Fig. 1 (The coordinates of the optimized structures are given as supplementary materials).

Effect of donor atom in 12, 15 and 18- member crown

Oxa-12C4 (12C4, I), which was designed and subsequently optimized has two donor O atoms placed diagonally at the top of the ring and two O atoms at the bottom of the ring. Geometries of aza (A12C4), thia (T12C4) and phospha (P12C4) are obtained by replacing one of the O atoms of the 12C4 with N, S and P donor atom respectively and their optimized structures are given in Fig. 1 (II-IV). The optimized

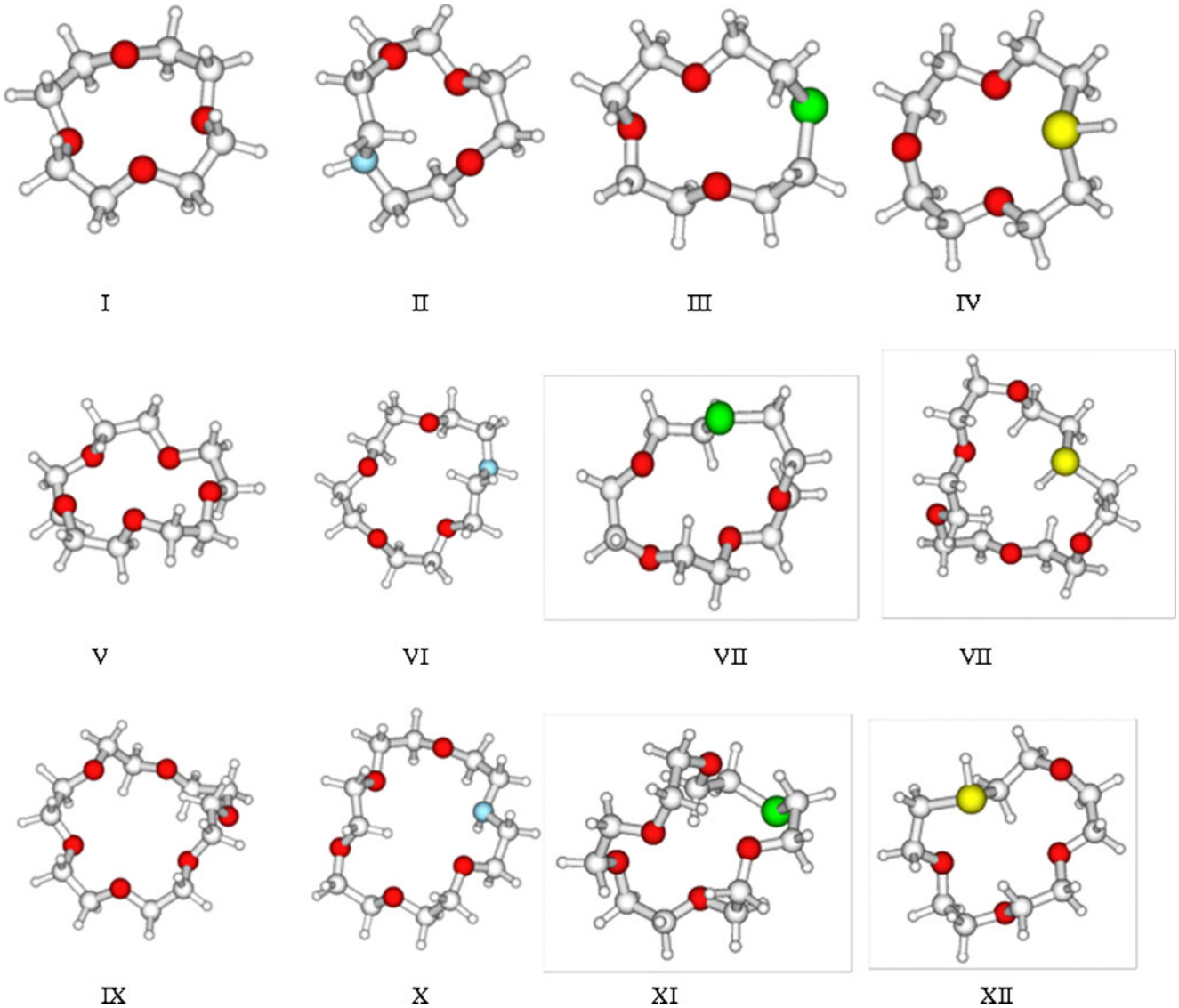

Fig. 1 Optimized geometries of unsubstituted free crown ether at MP2 level of theory using 6-311+G (d, p) basis set for oxa, aza, thia and phospha analogue of 12-crown-4 (I-IV), 15-crown-5 (V-VIII) and 18-crown-6 (IX-XII). The larger and small gray spheres represent the C and H atom respectively. The cyan, red, green and yellow color corresponds to N, O, S and P atom, respectively

minimum energy geometries of oxa, aza, thia and phospha crown of 15 member ring are displayed in Fig. 1 (V-VIII). In 15C5, 3 O donor atoms are lying above the plane of the crown ring and 2 O atoms are placed at the bottom of the crown ring. One of the bottoms placed O donor is replaced by N, S and P donor atom to make the aza, thia and phospha analog of 15C5. Fully relaxed structures of oxa, aza, thia and phospha crown of 18 member ring are also depicted in Fig. 1 (IX-XII). Three O atoms are lying above the plane of the crown ring and 3 O atoms are placed at the bottom of the crown plane. The calculated C-C, C-O and C-X (X-N, S and P) bond distances are presented in Table 1. The C-C (1.51 Å) and C-O (1.41-1.42 Å) bond distance remains almost unchanged. The C-X (X-N, S and P and C-N is 1.45-1.46 Å, C-S is 1.81 Å, C-P is 1.86-1.87 Å) bond distance is gradually increased from N donor to P donor atom as the size of the donor atom is increased within the crown ring. This structural change due to the donor atom has been reflected in the interaction profile of the lithium metal ion with the ligand (described in later section). The diagonally center to center O-X (X = O, N, P, S) minimum distance is given in Table 1 for all the crown ethers studied here. The O-X distance is increased in the following order: S>P>N>O in 12 member ring, whereas, in 15 member ring it follows: N>S>O>P and in 18 member ring: N>S>P>O. The donor atom has profound effect on the electronic charge distribution as clearly evident from the value of dipole moment given in Table 1. The dipole moment is increased with increase in the number of donor atom in the following order: 18C6>15C5>12C4 for different type of donor atoms considered here.

Table 1 Calculated values of C-C, C-O and C-X (X=N, S and P) bond length of crown ether at MP2 level of theory using 6-311+G (d,p) basis function

Crown system	C-C (Å)	C-O (Å)	C-X(X=N, S, P) (Å)	O-X (Å) (diagonally center-center distance)	Dipole moment (Debye)
a) 12C4, A12C4, T12C4 and P12C4					
12C4	1.513	1.415		3.806	0.00
A12C4	1.517	1.423	1.467	3.865	1.34
T12C4	1.515	1.412	1.819	4.868	1.56
P12C4	1.515	1.413	1.870	4.820	1.26
b) 15C5, A15C5, T15C5 and P15C5					
15C5	1.519	1.416		3.970	2.29
A15C5	1.515	1.415	1.461	4.882	1.95
T15C5	1.518	1.419	1.815	4.458	2.31
P15C5	1.519	1.418	1.864	3.545	2.82
c) 18C6, A16C6, T18C6 and P18C6					
18C6	1.512	1.414		5.118	2.31
A18C6	1.514	1.415	1.456	5.485	2.95
T18C6	1.516	1.413	1.819	5.460	2.56
P18C6	1.516	1.418	1.867	5.372	3.21

Effect of electronic induction on tuned 12 member crown

In order to tune the binding energy of the Li^+-ligand system, the electron density distribution of the phenyl substituted crown ring was perturbed by introducing different electron withdrawing and electron donating functional group. We have chosen 12C4 as the basic crown unit to study the effect of substitution of functional group as it contains fewer number of atoms in comparison to 15C5 and 18C6 ligand in view of large computational cost at MP2 level of theory. Also the cavity size of the 12C4 crown ether is just sufficient to accommodate the small size lithium ion of 0.6 Å radius. It will be interesting to study the effect of substitution on A12C4, T12C4 and P12C4 also. For the beginning we have started with 12C4. The optimized minimum energy structures of benzo substituted (B12C4) and electron withdrawing and donating group (Z) added to the benzene ring, Z-B12C4, where, Z=-NH_2, -CH_3, -$CONH_2$, -COOH, -CN and -NO_2 (Fig. 2). The C-C (1.52 Å) and C-O (1.44 Å) bond lengths are increased in comparison to free 12, 15 and 18 member crown ethers (Table 1 in supplementary materials). Further substitution of electron donating/withdrawing groups has a minimal effect on the cavity size of B12C4. The cavity size is highest in B12C4-CH3 (3.72 Å) and is lowest in B12C4-NH2 (3.56 Å), smaller by 0.16 Å than B12C4. The effect of donor, cavity and substituent on the electronic charge distribution can be visualize from the electrostatic surface charge density profile of the crown ligand as shown in Fig. 3. The value of dipole moment is increased due to substitution of benzene ring in 12C4. Further dipole moment is increased by introducing the electron withdrawing group on the benzene ring and is decreased by introducing electron donating group. The highest occupied molecular orbital (HOMO) of 12C4 is changed due to the additional substitution of benzene ring and electro donating methyl group in 12C4 moiety (Fig. 3). This electronic effect reduces the gap between HOMO and lowest unoccupied molecular orbital (LUMO) of B12C4-CH_3 (0.364 eV) in comparison to 12C4 (0.484 eV), which is manifested in their corresponding binding energy.

Metal crown ether complexes

Effect of donor atom on the structure of complexes of Li^+ ion with 12, 15 and 18 member ring

Optimized structures of lithium metal ion complexes with oxa, aza, thia and phospha crown of 12 member ring are displayed in Fig. 4 (I-IV). In Li^+-12C4 complex, donor O atom is aligned in alternate up and down order as was in free crown ether. Li metal ion is placed at the hydrophilic center of the crown ether. The optimized minimum energy structures of oxa, aza, thia and phospha crown of 15 member ring are displayed in Fig. 4 (V-VIII). In Li^+-15C5 complex, donor O atom is aligned as in free crown ether. Li metal ion is sited at the center of the crown ether. Optimized geometries of oxa, aza, and thia and phospha crown of 18 member ring are displayed in Fig. 4 (IX-XII). O atom is aligned in Li^+-18C6 complex like free crown ether. Li metal ion is fixed at the center of the crown ether. The C-C (1.51-1.52 Å) and C-O (1.42-1.44 Å) bond is slightly lengthened

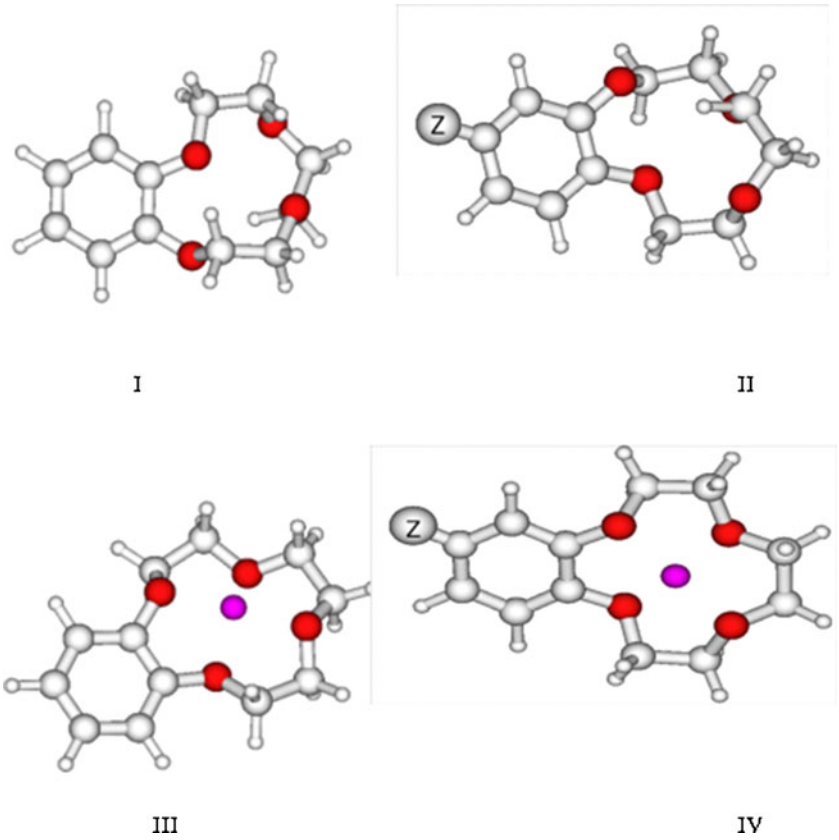

Fig. 2 Optimized geometries of benzo and functional group substituted crown ether and its Lithium complexes (I) Benzo-12-crown-4, (II) Z-B12C4, Z=NH_2, NO_2, COOH, CN, $CONH_2$ and CH_3. Key is same as in Fig. 1

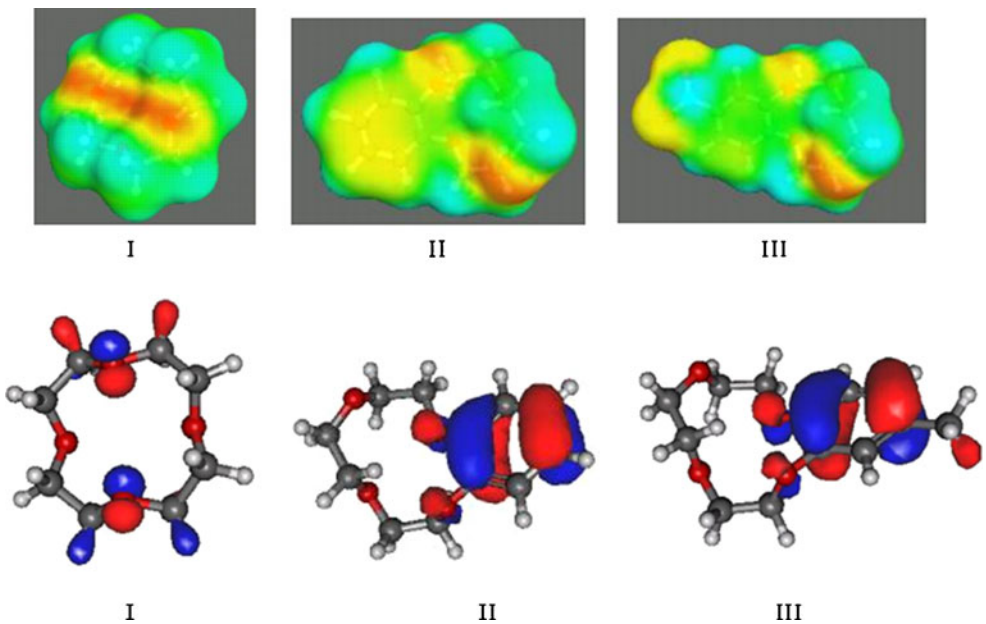

Fig. 3 Electrostatic surface charge density of crown ethers calculated at BP-86/TZVP level of theory and HOMO calculated at MP2/6-311+G(d,p) level of theory for (I) 12-crown-4, (II) Benzo-12-crown-4 and (III) CH3-Benzo-12-crown-4. Red color corresponds to the electron density rich region

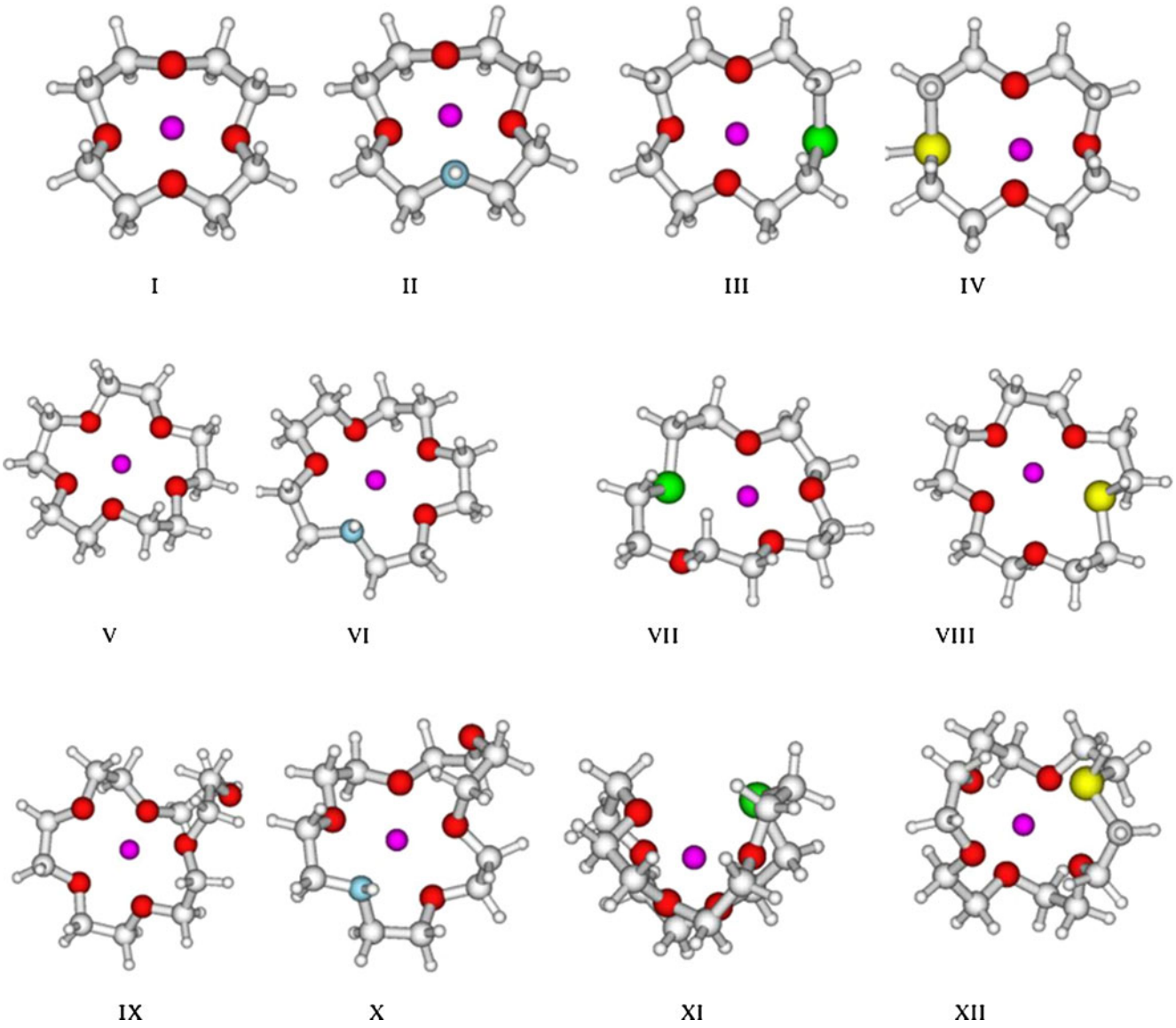

Fig. 4 Optimized geometries of unsubstituted Li^+-crown ether complexes at MP2 level of theory using 6-311+G (d, p) basis set for oxa, aza, thia and phospha analogue of Li^+-12-crown-4 (I-IV), Li^+-15-crown-5 (V-VIII) and Li^+-18-crown-6 (IX-XII). Violet sphere represents the Li atom. All other key is the same as in Fig. 1

due to complexation with the metal ion. The calculated Li-X (X=O, N, S and P) bond distances for 12, 15 and 18 member crown ligand are tabulated in Table 2. The Li-X bond distance is gradually increased with O, N, S and P donor atom within the crown ring with increase in the size of the donor atom. The maximum Li-X bond distance was found in P18C6 (2.752 Å) and lowest in 12C4 (1.869 Å) with aza and thia in between. The structure of the free crown ether is floppy in nature due to the repulsion between the lone pair electron of the donor atom. In presence of metal ion, the dipole of the donor atom is projected toward the metal ion in a definite manner which imparts rigidity to the crown skeleton and hence the ion-crown complex structure becomes rigid and symmetric. The size of the 18C6 (center-center diagonal O-O distance, 5.118 Å) is much higher than the size of the lithium ion (diameter: 1.2 Å). In order to satisfy the coordination number, Li metal ion (coordination number of lithium metal ion is 4) force the crown structure to be close to the O donor, which leads to a folded structure, where the Li ion is wrapped by the crown ether [71]. The Li-O bond becomes shorter due to this folded structure. The diagonally center to center O-O distance is decreased from free crown ether (12C4: 3.806 Å; 15C5: 3.970 Å; 18C6: 5.118 Å) after complexation with metal ion (12C4:3.536 Å; 15C5: 3.887 Å; 18C6: 3.739 Å) due to strong electrostatic interaction by the charge of the cation with the dipole offered by the donor crown ligand.

Table 2 Calculated values of C-C, C-X (X=O, N, S and P) and Li-X bond length of Li complexes of crown ether at MP2 level of theory using 6-311+G(d,p) basis function

Li- crown system	C-C (Å)	C-O (Å)	C-X(X=N, S, P) (Å)	Li-X (Å)	O-X (Å) (diagonally center-center distance)
a) 12C4, A12C4, T12C4 and P12C4					
12C4	1.523	1.440(1.44)[a]		1.869(2.02)[a]	3.536
A12C4	1.525	1.435(1.44)[a]	1.486(1.49)[a]	1.991(1.98)[a]	3.880
T12C4	1.522	1.436	1.838	2.385	4.296
P12C4	1.523	1.437	1.871	2.487	4.375
b) 15C5, A15C5, T15C4 and P15C5					
15C5	1.515	1.427		2.049	3.877
A15C5	1.517	1.425	1.465	2.252	4.194
T15C5	1.518	1.425	1.818	2.485	3.941
P15C5	1.513	1.434	1.869	2.491	3.851
c) 18C6, A18C6, T18C6 and P18C6					
18C6	1.513	1.422		2.009	3.739
A18C6	1.515	1.428	1.473	2.246	5.840
T18C6	1.519	1.430	1.816	2.620	3.857
P18C6	1.520	1.433	1.862	2.752	4.042

[a] calculated at B3LYP/6-31+G (d,P) level of theory, Ref [50]

Electronic induction effect on the tuned structure of 12C4

The optimized minimum energy structures of Li complexes of benzo substituted and attached electron withdrawing and donating group in B12C4 are displayed in Fig. 2. The C-C (1.52 Å), C-O (1.44 Å) and Li-O(1.89 Å) bond distance remains almost unchanged (see Table 2 of supplementary materials). The metal-ligand structure becomes more rigid and symmetric after complexation with Li metal ion. Diagonally center to center O-O distance (3.71 Å -3.72 Å in free crown ether) is decreased in the substituted crown ether with electron withdrawing and electron donating group after complexation with Li ion (3.49 Å -3.50 Å). This O-O diagonal distance in metal complexes of B12C4 and other substituted crown is nearly constant. There is no structural change but there is a

Table 3 Calculated values of binding energy for Li-crown ether complexes and chemical descriptors of free crown ether at MP2 level of theory using 6-311+G(d,p) basis function

System	BE kcal mol^{-1}	Charge on Li(a.u)	E_{HOMO} (eV)	E_{LUMO} (eV)	ΔE (eV)	χ	η	ΔN
a) 12C4, A12C4, T12C4 and P12C4								
12C4	-91.26 (-87.20)[a]	0.6324	-0.4054	0.0788	0.4842	0.1633	0.2421	0.4321
A12C4	-91.34 (-90.80)[a]	0.5486	-0.3602	0.068	0.4282	0.1461	0.2141	0.4458
T12C4	-90.32	0.6239	-0.3263	0.0732	0.3995	0.1265	0.1997	0.4566
P12C4	-86.50	0.6046	-0.3343	0.0654	0.3997	0.1344	0.1998	0.4539
b) 15C5, A15C5, T15C5 and P15C5								
15C5	-103.50	0.6103	-0.3999	0.0666	0.4665	0.1666	0.2332	0.4335
A15C5	-106.31	0.5939	-0.3572	0.069	0.4262	0.1441	0.2131	0.4468
T15C5	-97.60	0.6239	-0.3285	0.0614	0.3899	0.13355	0.19495	0.4557
P15C5	-92.76	0.4786	-0.3262	0.0648	0.3910	0.1307	0.1955	0.4565
c) 18C6, A16C6, T18C6 and P18C6								
18C6	-109.06	0.5465	-0.3986	0.0695	0.4681	0.1645	0.2340	0.4340
A18C6	-112.77	0.3724	-0.361	0.0657	0.4267	0.1476	0.2133	0.4455
T18C6	-113.69	0.4900	-0.3156	0.0615	0.3771	0.1270	0.1885	0.4599
P18C6	-108.31	0.3858	-0.3288	0.0592	0.3880	0.1348	0.1940	0.4556

[a] calculated at B3LYP/6-31+G (d,P) level of theory, Ref [50]

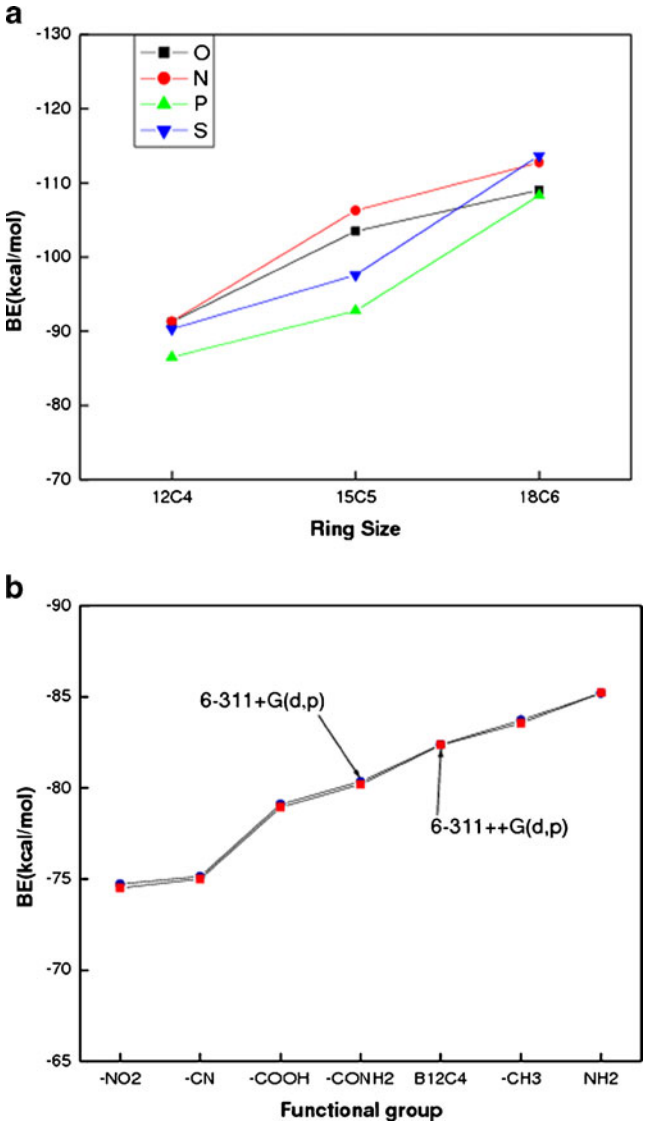

Fig. 5 Plot of binding energy (kcal mol^{-1}) versus ring size of the crown ether with different donor atom and different functional group attached B12C4 (**a**) Crown ether of different ring size with varied donor atom (**b**) B12C4 with different electron donating and electron withdrawing functional group using different basis set. The key is the same as in Fig. 1

change in the binding energy, which might be considered to be electronic origin in nature.

Binding energies

The calculated values of binding energy for 12 member ring are presented in Table 3 and Fig. 5a. The binding energy is found to be highest in A12C4 (-91.34 kcal mol^{-1}) and lowest in P12C4 (-86.50 kcal mol^{-1}). Oxa (-91.26 kcal mol^{-1}) and aza are of very close value. The biding energy order is obtained as: A12C4~12C4>T12C4>P12C4. The interior of the crown ligand acts as a hydrophilic and the exterior of the crown ether acts as a hydrophobic region as the electron density is mainly projected to the center of the crown ring as clearly seen in the electrostatic potential of the 12C4 ligand (Fig. 3). Also, in the case of 15 member ring the binding energy order is the same as in 12 member series. The binding energy in A15C5 is higher by 13.55 kcal mol^{-1} than that of P15C5. The binding energy order is changed in the case of 18 member ring. The binding energy order is T18C6~A18C6> 18C6~P18C6. This may be due to the higher charge transfer in thia crown than the oxa crown ether. The binding energy in T18C6 (-113.69 kcal mol^{-1}) is more by 16.08 kcal mol^{-1} than that of T15C5 (–97.60 kcal mol^{-1}). The binding energy in T18C6 is very close to the value of A18C6 (-112.77 kcal mol^{-1}). The binding energy is increased by 6.5% in A18C6 compared to A15C5. O18C6 (-109.06 kcal mol^{-1}) and P18C6 (-108.31 kcal mol^{-1}) are of very close value. All the crown ether studied here, the binding energy for oxa and aza are very close, whereas thia and phospha are very close to each other. The binding energy is increased from A12C4 to A15C5 by 17.94% and for A15C5 to A18C6 by 6.5% whereas in case of oxa, the corresponding increment is 14.68% and 5.82% respectively. In going from 12 to 15 member ring, for both oxa and aza there is a jump in binding energy, but no such jump is noticed in corresponding thia and phospha crown. Whereas jump in binding energy is observed from 15C5 to 18C6 (16 kcal mol^{-1}) for both thia and

Table 4 Calculated values of binding energy of Li^+-B12C4 complexes with various functional group attached to B12C4 and chemical descriptors of corresponding free ligand at MP2 level of theory using 6-311+G(d,p) basis function

System	BE kcal mol^{-1}	Charge on Li (a.u)	E_{HOMO} (eV)	E_{LUMO} (eV)	ΔE (eV)	χ	η	ΔN
B12C4	-82.38	0.7512	-0.3077	0.0652	0.3729	0.1212	0.1864	0.4625
B12C4-NH_2	-85.21	0.7563	-0.2828	0.0653	0.3481	0.1087	0.1740	0.4706
B12C4-NO_2	-74.72	0.7768	-0.3417	0.0426	0.3843	0.1495	0.1921	0.4512
B12C4-COOH	-79.11	0.7389	-0.3233	0.0621	0.3854	0.1306	0.1927	0.4574
B12C4-CN	-75.14	0.7406	-0.329	0.056	0.3850	0.1365	0.1925	0.4555
B12C4-$CONH_2$	-80.34	0.7669	-0.3202	0.0592	0.3794	0.1305	0.1897	0.4584
B12C4-CH_3	-83.72	0.7495	-0.2988	0.0652	0.3640	0.1168	0.182	0.4654

phospha but no such jump is observed for oxa and aza crown ether. In 18C6 analogue of thia and phospha, the thia and phospha donor atom push the O atoms toward central Li metal ion keeping itself far from the ion and hence leads to a folded structure. The effect of benzo substitution and different electron withdrawing and electron donating group on Li^+-12C4 binding energy is given in Table 4 and Fig. 5b. The electronic inductive effect caused by the substitution of electron withdrawing and electron donating group either enhance or deplete the electron density on the pi electron of the benzene moiety. The electron withdrawn group, viz. $–NO_2$, -COOH, $-CONH_2$ and -CN (-ve inductive effect) reduces the electron density on the benzene ring which in turn reduces the electron density on the crown moiety and hence the binding energy with metal ion is reduced. Similarly, the electron donating group (+ve inductive effect) enhances the electron density on the crown moiety via benzene ring and hence leads to the increase in binding energy with the metal ion. The charge density distribution takes place via intra-molecular charge transfer between the functional substituent and the phenyl ring attached to the crown ring. The binding energy is highest in amine substituted B12C4 (-85.21 kcal mol^{-1}) and lowest in nitro substituted B12C4 (-74.72 kcal mol^{-1}). The binding energy order is B12C4-NH_2> B12C4-CH_3> B12C4> B12C4-$CONH_2$~B12C4-COOH> B12C4-CN~ B12C4-NO_2. The results demonstrate that the binding energy can be significantly tuned through the introduction of suitable substituent or functional group. The partial charge transfer was calculated using CHelpG scheme. No correlation was found between the binding energy and partial charge transfer. The binding energy was also calculated using 6-311++G (d,p) basis set at MP2 level of theory and it is seen that there is very small change in the binding energy using large basis set (see Fig. 5b). To further test the effect of basis set, we performed the BSSE correction using full counterpoise method [72] and the calculated values are presented in Table S3. The BSSE corrected binding energy was found to be overestimated at the present MP2 level of theory with frozen core approximation [40].

Quantum chemical descriptors

The calculated values of HOMO and LUMO energies, energy gaps, absolute hardness (η), absolute electro negativity (χ) and charge transfer, ΔN of the optimized crown ligand – metal ion systems are given in Table 3 and 4. The HOMO-LUMO energy gaps are decreased gradually from 12C4 to T12C4 which implies that the hardness of the donor ligand is decreased from 12C4 to T12C4. The ΔE (HOMO-LUMO) is large for N and O based ligand and small for P and S based ligand, suggesting the hard and soft donating ability. The hardness parameter is high for N(0.21) and O (0.24) but small for S and P donor ligand. Here, the ΔE (HOMO-LUMO) follows the order O>N>P>S. Lithium ion being a hard acid will give stable complexes with hard bases, i.e., with O and N based ligand and the same is obtained from the present calculation. In the case of 15 member ring crown ether, the HOMO-LUMO energy gap is decreased slightly in comparison to the 12 member ring. Here, the ΔE (HOMO-LUMO) follows the order O>N>S>P. The ΔE (HOMO-LUMO) follows the order O>N>S>P in the case of 18 member crown ether. The 12C4 moiety is then tuned with benzene ring. The HOMO-LUMO gap is reduced in comparison to the parent 12C4 moiety due to electron withdrawing effect of benzene ring which indicates the higher reactivity of the molecule. The B12C4 is further modified with electron donating and electron withdrawing functional group. The calculated values of HOMO-LUMO gap is presented in Table 4. The ΔE (HOMO-LUMO) follows the order B12C4-COOH> B12C4-CN> B12C4-NO_2> B12C4-$CONH_2$> B12C4-CH_3> B12C4-NH_2. As observed earlier, 12C4 has the largest energy gap among the homologues and hence most stable. In order to calculate the fractions of electron transferred from the donor crown ether to the metal ion, theoretical values for absolute electronegativity and absolute hardness for Li metal ion was calculated. The theoretical value of absolute electronegativity of Li metal ion is 1.49 eV and absolute hardness is 1.29 eV.

According to Pearson's HSAB principle, hard acids prefer to bind hard bases and soft acids prefer to bind soft bases. Crown ether ligand with oxygen and nitrogen as donor atom acts as a hard base as evident from high energy HOMO and high values of hardness (η) and electro negativity (χ). Hence in accordance with the HSAB principle Aza-crown ether prefers Li metal ion over other crown ether during complexation.

A large value of ΔN is favorable for a donor-acceptor reaction. The value of ΔN is higher for B12C4-NH_2-Li^+ system (0.047) and lowest for B12C4-NO_2-Li^+ system (0.045), which indicates that the complexation with B12C4-NH_2 is more favorable than B12C4-NO_2. The fraction of electron transferred is largest for B12C4-NH_2 followed by B12C4-CH_3> B12C4-$CONH_2$> B12C4-COOH> B12C4-CN> B12C4-NO_2. From Mulliken population analysis it was found that the charge transfer was highest for B12C4-NH_2 followed by B12C4-CH_3> B12C4-COOH> B12C4-$CONH_2$> B12C4-CN> B12C4-NO_2. The binding energy of functional group modified crown ether is well correlated with the fraction of electron transfer, ΔN but cannot be correlated with the ChelpG partial charge transfer.

Thermodynamic parameters

The calculated values of zero point and thermal corrected binding energy along with binding enthalpy, free energy of

Table 5 Calculated thermodynamic parameters Li^+-crown ether systems at MP2 level of theory using 6-311+G(d,p) basis function. The temperature considered here was 298.15 K

System	ΔU kcal mol^{-1}	ΔH kcal mol^{-1}	ΔS kcal mol^{-1}/K	ΔG kcal mol^{-1}
12 member crown ether				
12C4	-85.35	-84.76	-0.037	-73.69
A12C4	-86.17	-85.58	-0.030	-76.51
T12C4	-83.81	-83.22	-0.030	-74.36
P12C4	-80.21	-79.62	-0.029	-71.00
15 member crown ether				
15C5	-98.30	-97.71	-0.030	-88.88
A15C5	-100.86	-100.26	-0.032	-90.81
T15C5	-92.78	-92.19	-0.029	-83.67
P15C5	-87.23	-86.64	-0.025	-79.11
18 member crown ether				
18C6	-102.68	-102.09	-0.036	-91.30
A18C6	-105.94	-105.35	-0.037	-94.31
T18C6	-107.79	-107.20	-0.032	-97.75
P18C6	-102.48	-101.89	-0.043	-88.93

complexion and entropy of complexion (ΔS) are listed in Table 5 and 6. These thermodynamic values provide information about the relative stability of crown ether complexes. Formation of metal ion complexes is exothermic as revealed from values of ΔH given in Table 5 and 6. The zero point energy and thermodynamically corrected binding energy are calculated from the Hessian of the optimized geometry. The binding enthalpy is highest for A12C4 (-85.58 kcal mol^{-1}) and lowest for P12C4 (-79.62 kcal mol^{-1}). The binding enthalpy order is similar like binding energy, i.e., A12C4~12C4>T12C4>P12C4. The binding enthalpy is increased with increase in the cavity size, i.e., with increase in number of O atoms. In the case of 15 member crown ring, the binding enthalpy order is the same as observed in 12 member ring. The binding enthalpy in A15 C5 is higher by (2.55 kcal mol^{-1}) than that of oxa, by (8.07 kcal mol^{-1}) than thia and by (13.62 kcal mol^{-1}) than phospha. The binding enthalpy order is changed in the case of 18 C6 and the order is A18C6~T18C6>18 C6~P18C6. In 18 member ring, the entire crown with different donor atom has very close binding enthalpy within 5 kcal mol^{-1}. The thia analogue has the highest binding enthalpy (-107.20 kcal mol^{-1}) and phospha has the lowest binding enthalpy (-101.89 kcal mol^{-1}). The phospha crown in all 12, 15 and 18 member rings has the lowest binding enthalpy. The binding enthalpy is decreased due to substitution of electron withdrawing benzene ring. The binding enthalpy of functional group attached B12C4 revealed an interesting observation. Amine substituted B12C4 (-68.56 kcal mol^{-1}) has the lowest binding enthalpy though it has the highest binding energy (-85.21 kcal mol^{-1}). This is attributed to high zero point energy contribution. The methyl substituted B12C4 has the highest binding enthalpy (-76.35 kcal mol^{-1}). The free energy change for binding the metal ion is also highest for B12C4-CH_3. The entropy change for the complexation reaction is slightly negative because it is a structure making process. However, the change in the enthalpy was large and negative enough to overcome the negative entropy change. From the free energy of complexation it is found that the metal ion-crown ether complexes are readily formed and stable.

Solvent exchange reaction

The calculated values of reaction enthalpy and reaction free energy against no water molecules are plotted in Fig. 6a-c. From the figure it is seen that the enthalpy of reaction is negative up to four water molecules and then it turns positive which means that after four water molecules the reaction is not feasible; but here, entropy plays the vital role. With the addition of more water molecules the entropy becomes more positive due to randomness of the free water molecules after dehydration of the water molecules due to complexation with the ligand and resulted in the negative free energy of complexation. After four water molecules the free energy of the reaction reaches a plateau which incidentally is the first shell coordination number of lithium ion.

Table 6 Calculated thermodynamic parameters of Li^+-crown ether systems at MP2 level of theory using 6-311+G (d,p) basis function. The temperature considered here was 298.15 K

System	ΔU kcal mol^{-1}	ΔH kcal mol^{-1}	ΔS kcal mol^{-1}/K	ΔG kcal mol^{-1}
B12C4	-78.52	-77.93	-0.034	-67.70
B12C4-NH_2	-69.15	-68.56	-0.039	-56.79
B12C4-NO_2	-70.52	-69.92	-0.030	-60.87
B12C4-COOH	-74.91	-74.32	-0.030	-65.29
B12C4-CN	-71.01	-70.41	-0.030	-61.42
B12C4-$CONH_2$	-76.25	-75.66	-0.030	-66.72
B12C4-CH_3	-79.15	-76.35	-0.031	-69.26

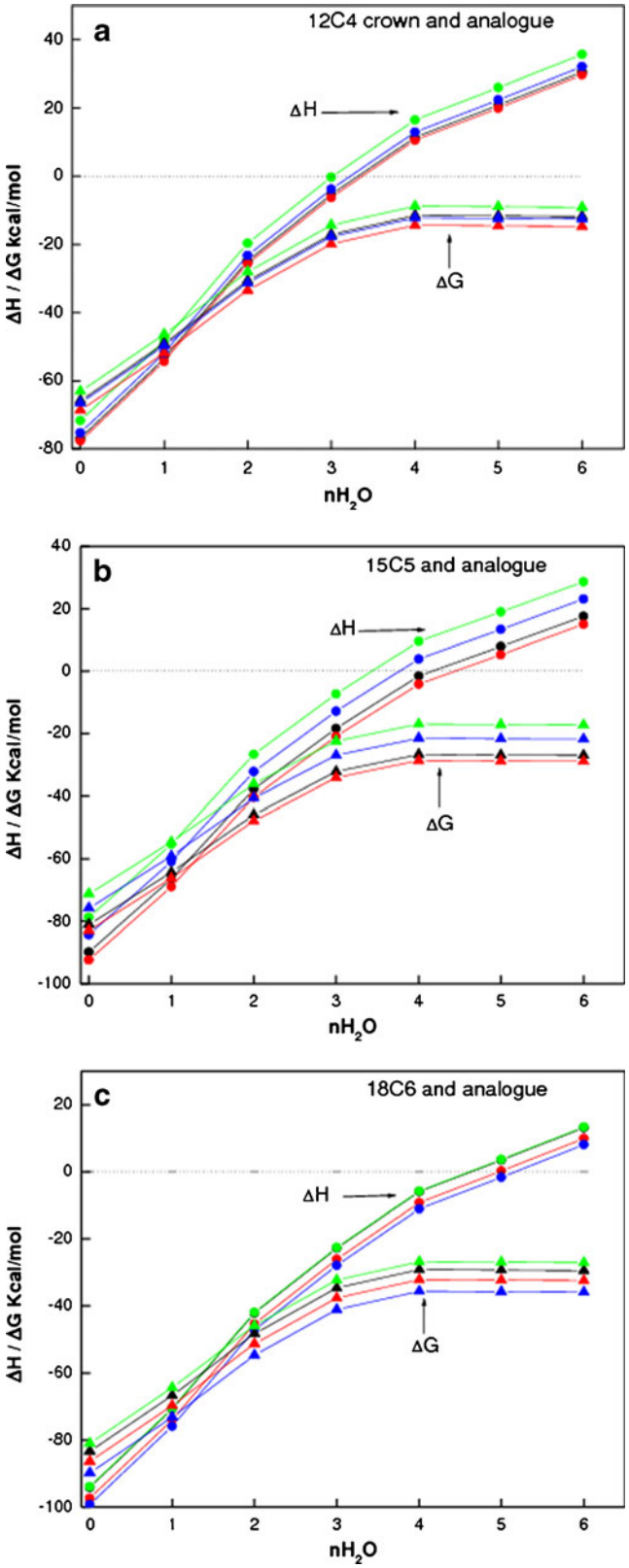

Fig. 6 Plot of enthalpy, ΔH and free energy, ΔG (kcal mol^{-1}) of solvent exchange reaction (Eq. 14) with crown ligand against number of water molecules (nH_2O, n=1-6). (**a**) 12 member (**b**) 15 member (**c**) 18 member. Red, black, blue and green color corresponds to N, O, S and P donor based ligand respectively. The key is the same as in Fig. 1

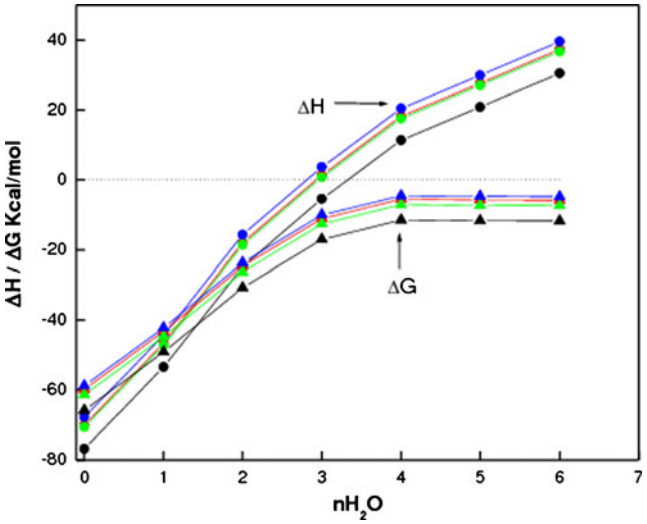

Fig. 7 Plot of enthalpy, ΔH and free energy, ΔG (kcal mol^{-1}) of solvent exchange reaction (Eq. 14) with functional group substituted crown ligand against number of solvent water molecules (nH_2O, n=1-6). Black, red, green and blue color corresponds to 12C4, B12C4, B12C4-CH_3 and B12C4-$CONH_2$ ligand respectively. The key is the same as in Fig. 1

The highest enthalpy of reaction is shown by aza crown and lowest by phospha crown ether. Point to be noted that both the reaction enthalpy and reaction free energy are lowered due to the presence of solvent water molecules. Similar observation was found in the case of 15 member crown ring also as shown in Fig. 6b. In the case of 18 member crown ring there is a change in the trend of free energy. The thia analogue has the highest free energy of reaction and the phospha crown has the lowest free energy of reaction as shown in Fig. 6c. This is because of the entropy change which, in the case of thia is lower than phospha crown ether. It is interesting to see the effect of water molecules on the binding energy of metal ion with substituted 12C4. The calculated values of enthalpy and free energy change with water molecules are plotted in Fig. 7. The value of binding enthalpy is decreased due to substitution of benzo group in the 12C4 ring. Further, addition of electron withdrawn group is resulted in lower binding enthalpy and addition of electron donating group resulted in higher binding enthalpy. Here, also the binding enthalpy becomes positive after four water molecules but positive entropy contribution due to release of water molecules during complexation resulted in negative free energy, which facilitates the complexation reaction.

Solvent effect on the structural and energetic parameters

Practically most of the separation process occurs from aqueous environment to the organic phase. So it is worthwhile to

explore the effect of the solvent on the structure of the ligand and energetic. In view of this we have optimized the structure of B12C4 in nitrobenzene (NB), chloroform ($CHCl_3$) and carbon tetrachloride (CCl_4) using COSMO formalism at BP86-TZVP level of theory. The structural parameters of B12C4 in gas, NB, $CHCl_3$ and CCl_4 phase are presented in Table 7. There is no significant change in the C-C (1.51-1.52 Å) and C-O (1.43 Å) bond length. The HOMO-LUMO gap is decreased gradually from gas phase to organic solvent phase with increasing solvent dielectric constant. The dipole moment of B12C4 in gas phase is increased from 1.29 to 1.58 Debye in CCl_4, 1.79 Debye in $CHCl_3$ and 2.06 Debye in NB. The increment in dipole moment arises due to the polarization of the crown molecule by polar organic solvent. The order of dipole moment follows the order of polarity (dielectric constant, ε) of the organic solvent as: ε_{NB}(34.81)> ε_{CHCl3}(4.82)> ε_{CCl4}(2.24). The gas phase binding energy is reduced in solvent phase as the polar solvent molecules weaken the metal-ligand binding. The calculated value of solvation energy also follows the order of solvent polarity.

The calculated values of extraction energy for the solvent extraction reaction (Eq.(12)) are given in Table 7. The extraction energy in NB (-12.27 kcal mol^{-1}) phase is higher in comparison to the $CHCl_3$ (-8.036 kcal mol^{-1}) and CCl_4 (-4.17 kcal mol^{-1}) phase due to higher dielectric constant of NB, means NB is a better solvent than $CHCl_3$ and CCl_4 for LiCl salt extraction from aqueous phase.

imilar calculation was also performed for B12C4-CH_3 ligand in NB solvent. Here also, the HOMO-LUMO gap is decreased and dipole moment is increased from gas phase to NB phase. The extraction energy is more in comparison to B12C4 due to the electron donating methyl group in the benzene ring. To validate this theoretical prediction we carried out a solvent extraction experiment given in subsequent section.

Solubility and partition coefficients

The solubility of ligand in water and its partitioning in the water–solvent bi-phasic system plays the crucial role in the use of it in different solvent extraction based technology. The designer ligand should have a low aqueous solubility and high partition coefficient to have an economical and efficient solvent extraction based process design. The calculated values of solubility of the designed crown ether are tabulated in Table S4 (supplementary). From the table it is seen that the A12C4 has the highest and T12C4 has the lowest solubility in water. The solubility follows the order A12C4>P12C4>O12C4>T12C4. The solubility of 15C5 is increased due to extra ether linkage. There is a marked increase in the solubility of A15C5, whereas the solubility is reduced for P15C5 and T15C5. The aqueous solubility of 18C6 is higher than 15C5 member ring except P18C6, where it is increased. Aza family crown studied here has the highest aqueous solubility. So its use in solvent extraction experiment is not recommended. Addition of benzene ring to the 12C4 reduces the aqueous solubility. Further tuning of B12C4 with functional group like NH_2, NO_2, COOH, CN, $CONH_2$ increases the solubility in water, whereas methyl substitution to phenyl ring decreases the aqueous solubility due to increased hydrophobicity. Hence, B12C4-CH_3 ligand appears to be the suitable ligand for extraction of Li ion.

In view of the role of the organic solvent, the partition coefficient of crown ligand in water-organic biphasic system is calculated and the data are given in Table S4 (supplementary). In the case of 12C4 series, T12C4 (3.63) has the highest partition coefficient in $CHCl_3$ and lowest in CCl4 (1.79). This might be due to the high dielectric constant of $CHCl_3$ compared to CCl_4. The order is as follows: $CHCl_3$>NB>CCl4. The highest partition coefficient was found for P15C5 (3.91) in the 15C5 series in $CHCl_3$ solvent. In the case of 18C6 series, T18C6 (4.59) has the highest partition coefficient in $CHCl_3$. Benzo substituted 12C4

Table 7 Calculated structural and energy parameters of B12C4 and B12C4-CH_3 in gas and solvent phase at BP-86 level of theory using TZVP basis set

Phase	C-C (Å)	C-O (Å)	HOMO-LUMO (eV)	Dipole moment (Debye)	Solvation energy kcal mol^{-1}	BE kcal mol^{-1}	E_{ex} kcal mol^{-1}	K_d (Exp)
a) B12C4								
Gas	1.5233	1.4323	4.18	1.29	-	-71.07	-	-
NB	1.5223	1.4348	4.15	2.06	-7.89	-7.80	-12.27	$3.08x10^{-3}$
$CHCl_3$	1.5191	1.4321	4.16	1.79	-5.63	-25.33	-8.036	$4.76x10^{-5}$
CCl_4	1.5195	1.4314	4.17	1.58	-3.45	-44.56	-4.17	$2.67X10^{-5}$
b) B12C4CH_3								
Gas	1.5164	1.4344	4.05	1.14	-	-78.12	-	-
NB	1.5190	1.4285	4.02	1.85	-7.87	-10.93	-12.43	-

(4.63) has the highest partition coefficient of all the unsubstituted due to increased hydrophobicity with the addition of extra benzene ring. The B12C4 crown moiety is further tuned with the different electron withdrawing and electron donating functional group attached to the benzene ring. Among the different functional group substituted B12C4, methyl substituted crown ether has the highest partition coefficient in $CHCl_3$ (5.2) again due to enhanced hydrophobicity of B12C4 due to the addition of methyl group. The partition coefficient of B12C4 (3.82) and B12C4-CH_3 (4.89) are high also in NB solvent. In 12 member series, B12C4 and B12C4-CH_3 are found to be the suitable ligands in view of their low aqueous solubility and high partition coefficient in $CHCl_3$ and nitrobenzene, and also due to their high binding enthalpy and extraction energy for extraction of LiCl solution.

The value of distribution coefficient obtained from the experiment is given in Table 7. The partitioning of LiCl is higher in NB than in $CHCl_3$ and CCl_4 due to its dielectric constant and the same trend was predicted from the theoretical calculation.

Conclusions

The present work reports the various structural, energetic and thermodynamical parameters for crown ether ligand-Li complex system at MP2 and DFT level of theory in gas as well as in solvent phase. The binding energy of lithium ion depends on the type of donor atom, cavity size and electron withdrawing and electron donating functional group in the crown ligand. The binding energy/enthalpy order found in 12C4 is A12C4~O12C4>T12C4>P12C4. In the case of 15 member ring also the same order is followed. The binding energy/enthalpy order is changed in the case of 18 member ring. The order is A18C6~T18C6>O18C6~P18C6. For a given donor type the binding energy is increased due to increase in the donor atom due to dipole-charge electrostatic interaction. The binding energy/enthalpy is decreased due to the electron withdrawing benzo substitution and it is further altered by introducing different electron withdrawing and electron donating groups in the benzene ring. The binding energy is highest in amine substituted B12C4 and lowest in nitro substituted B12C4. The binding energy order is B12C4-NH_2> B12C4-CH_3~ B12C4> B12C4-$CONH_2$~ B12C4-COOH> B12C4-CN~ B12C4-NO_2. The binding energy of functional group modified crown ether is well correlated with the fraction of electron transfer, ΔN but cannot be correlated with Mulliken charge transfer. The free energy change for binding the metal ion is highest for B12C4-CH_3. The entropy change for the complexation reaction is slightly negative. However, the change in the enthalpy was large and negative enough to overcome the negative entropy change. From the free energy of complexation it is found that the metal ion-crown ether complexes are readily formed and stable. There is no significant change in the C-C and C-O bond length and in HOMO-LUMO gap from gas phase to organic phase. The gas phase binding energy is reduced in solvent phase as the polar solvent molecules weaken the metal-ligand binding. The extraction energy in NB phase is higher in comparison to the $CHCl_3$ and CCl_4 phase due to higher dielectric constant of NB, means NB is a better solvent for LiCl salt extraction from aqueous phase. In 12 member series, B12C4 and B12C4-CH_3 are found to be the suitable ligands in view of their high extraction energy, low aqueous solubility and high partition coefficient in nitrobenzene.

Future studies will include Li^+ complexation studies with substituted A12C4, T12C4 and P12C4. Also studies can be carried out with bezo substituted 15C5, because from this study, it has been observed that for benzo substitution the C-O bond lengths are increased from 1.41 to 1.44 Å in the case of 12C4. So, if one can substitute two benzo groups on 15C5, it will further increase the C-O bond lengths which means a decrease in the cavity of crown ether and can be further reduced by different substitution. Another interesting study will be to investigate the donor effect on the IR spectra of the hydrated metal ion-crown system [73]. The systematic study presented here should contribute to the design of host ligand and screening of solvent for metal ion recognition and thus can contribute to plan the experiments.

Acknowledgments We would like to acknowledge the computer division of the Bhabha Atomic Research Centre for the ANUPAM super computational facility.

References

1. Villani, S (1976) Isotope separation. American Nuclear Society
2. Symons EA (1985) Sep Sci Technol 20:633–651
3. Briant RC, Weinberg AM (1957) Nuclear science and engineering 2:797–803
4. Glasstone S, Sesonkse A (1994) Nuclear reactor engineering. Chapman and Hall, London
5. Ehrlich BE, Diamond JM (1980) J Membrane Biol 52:187–200
6. Berridge MJ, Irvine RF (1989) Nature 341:197–205
7. Shikama T, Knitter R, Konys J, Muruga T, Tsuchya K, Moeslang A, Kawamura H, Nagata S (2008) Fusion Eng Des 83:976–982
8. Heumann KG (Ed) (1985) Topics in Current chemistry, 127, Springler, Berlin
9. Nishizawa K, Takano T, Ikeda I, Okahara M (1988) Sep Sci Technol 23:333–343
10. Pederson CJ (1967) J Am Chem Soc 89:7017–7036
11. Lemaire M, Guy A, Chomelcand R, Foos J (1991) J Chem Soc Chem Commun 1152-1154
12. Kim DW, Kang BM, Jeon BK, Jeon YS (2003) J Rad Nu Chem 256:81–85
13. Kanzaki Y, Suzuki N, Chitrakar R, Ohsaka T, Abe M (2002) J Phys Chem B 106:988–995

14. Sannicolo F, Brenna E, Benincori T, Zotti G, Zecchin S, Schiavon G, Pilati T (1998) Chem Mater 10:2167–2176
15. Tokunaga Y, Nakamura T, Yoshioka M, Shimomura Y (2006) Tetrahedron Lett 47:5901–5904
16. Mathias LJ (1981) J Macromol Sci Chem A 15:853–876
17. Wipff G, Weiner P, Kollman P (1984) J Am Chem Soc 104:3249–3258
18. Hancock RD (1990) Acc Chem Res 23:253–257
19. Howard AE, Singh UC, Billeter M, Kollman PA (1998) J Am Chem Soc 110:6974–6984
20. Van Eerden J, Harkema S, Fed D (1988) J Phys Chem 92:5076–5083
21. Straatsma TP, McCammon JA (1989) J Chem Phys 91:3631–3637
22. Dang LX, Kollman P (1990) J Am Chem Soc 112:5716–5720
23. Sun Y, Kollman PA (1992) J Chem Phys 97:5108–5118
24. Leuwerink FTH, Harkema S, Briels WJ, Feil DJ (1993) Comput Chem 14:899–906
25. Ha YL, Chakraborty AK (1991) J Phys Chem 95:10781–10787
26. Ha YL, Chakraborty AK (1993) J Phys Chem 97:11291–11299
27. Hay BP, Rustad JR (1994) J Am Chem Soc 116:6316–6326
28. Ranghino G, Romano S, Lehn JM, Wipff G (1985) J Am Chem Soc 107:7873–7877
29. Jagannadh B, Jagarlapudi A, Sarma RP (1999) J Phys Chem A 103:10993–10997
30. El-Azhary AA, Al-Kahtani AA (2004) J Phys Chem A 108:9601–9607
31. Seidl ED, Schaefer HF III (1991) J Phys Chem 95:3589–3590
32. Wasada H, Tsutsui Y, Yamane S (1996) J Phys Chem 100:7367–7371
33. Hill SE, Feller D, Glendenning ED (1998) J Phys Chem 102:3813–3819
34. Yamabe T, Hori K, Akagi K, Fukui K (1979) Tetrahedron 35:1065–1072
35. Hori K, Yamada H, Yamabe T (1983) Tetrahedron 39:67–73
36. Ha YL, Chakraborty AK (1992) J Phys Chem 96:6410–6417
37. Glendening ED, Feller D, Thompson MA (1994) J Am Chem Soc 116:10657–10669
38. Glendening ED, Feller D (1996) J Am Chem Soc 118:6052–6059
39. Feller D (1997) J Phys Chem A 101:2723–2731
40. Feller D, Apra E, Nichols JA, Bernholdt DE (1996) J Chem Phys 105:1940–1950
41. Feller D, Thompson MA, Kendall RA (1997) J Phys Chem A 101:7292–7298
42. Cui C, Cho SJ, Kim KS (1998) J Phys Chem A 102:1119–1123
43. Tossel JA (2001) J Phys Chem B 105:11060–11066
44. Puchta R, van Eldik R (2007) EJIC 1120-1127
45. De S, Boda A, Ali SM (2010) J Mol Struct (THEOCHEM) 941:90–101
46. Boda A, Ali SM, Shenoi MRK, Rao H, Ghosh SK (2011) J Mol Model 17:1091–1108
47. Hori K, Inoue T, Tsukube H (1996) Tetrahedron 52:8199–8208
48. Okano K, Tsukube H, Hori K (2004) Tetrahedron 60:10877–10882
49. Diao KS, Wang HJ, Qiu JM (2009) J Mol Struct (THEOCHEM) 901:157–162
50. Diao KS, Bai LJ, Wang HJ (2011) Comput Theor Chem 964:18–24
51. Krishnan R, Pople JA (1978) Int J Quantum Chem 14:91–100
52. Ray D, Feller D, More MB, Glendening ED, Armentrout PB (1996) J Phys Chem 100:16116–16125
53. Boulatov R, Du B, Meyers EA, Shore SG (1999) Inorg Chem 38:4554–4558
54. Schmidt MW, Baldridge KK, Boatz JA et al (1993) J Comput Chem 14:1347–1363
55. Schaftenaar G, Noordik JM (2000) J Comput Aided Mater Des 14:123–134
56. Scotto MA, Mallet G, Vasilescu D (2005) J Mol Struct (THEOCHEM) 728:231–242
57. Parr RG, Yang W (1989) Density functional theory of atom and molecules. Oxford University Press, New York
58. TURBOMOLE is program package developed by the Quantum Chemistry Group at the University of Karlsruhe, Germany, 1988. Ahlrichs R, Bar M, Haser M, Horn H, Kolmel C (1989) Chem Phys Lett 162:165-169
59. Becke AD (1988) Phys Rev A 38:3098–3100
60. Perdew JP (1986) Phys Rev B 33:8822–8824
61. Eckert F, Klamt A (2008) COSMOtherm, version C2.1, Release 01.08. COSMOlogic GmbH & CoKG. Leverkusen, Germany
62. Klamt A (2005) COSMO-RS from quantum chemistry to fluid phase thermodynamics and drug design. Elsevier, Amsterdam
63. Klamt A (1995) J Phys Chem 99:2224–2235
64. Eckert F, Klamt A (2002) Am Inst Chem Eng J 48:369–385
65. Klamt A, Eckert F (2004) Fluid Phase Equilib 172:43–72
66. Putnam R, Taylor R, Klamt A, Eckert F, Schiller M (2003) Ind Eng Chem Res 42:3635–3641
67. Klamt A, Eckert F, Hornig M (2001) J Comput Aided Mol Des 15:355–365
68. Klamt A (2003) Fluid Phase Equilib 206:223–235
69. Pearson RG (1988) Inorg Chem 27:734–740
70. Parr RG, Pearson RG (1983) J Am Chem Soc 105:7512–7516
71. Haya BM, Hurtado P, Hortel AR, Hamad S, Steill JD, Oomens J (2010) J Phys Chem 114:7048–7054
72. Boys SF, Bernardi F (1970) Mol Phys 19:553–556
73. Rodriguez JD, Vaden TD, Lisy JM (2009) J Am Chem Soc 131:17277–17288